ChemComm

Accepted Manuscript

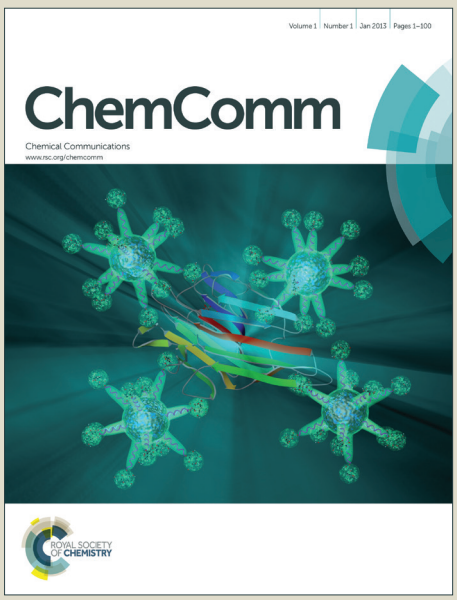

ROYAL SOCIETY OF CHEMISTRY

www.rsc.org/chemcomm

Cite this: DOI: 10.1039/c0xx00000x

www.rsc.org/xxxxxx

COMMUNICATION

Investigating nanoparticles properties in plasmonic nanoarchitectures with DNA by Surface Plasmon Resonance imaging

Stefano Mariani,[a] Simona Scarano,[a] Maria Laura Ermini,[a] Massimo Bonini[a,b]* and Maria Minunni[a,b]*

Received (in XXX, XXX) XthXXXXXXXXX 20XX, Accepted Xth XXXXXXXXX 20XX

DOI: 10.1039/b000000x

Nanoparticles with different sizes, refractive indices and plasmonic profiles are synthesized, labelled to DNA and embedded in DNA based plasmonic nanoarchitectures. The contributions of the different properties on Reflectivity Variations % are rationally investigated by DNA hybridization measurements with Surface Plasmon Resonance imaging (SPRi) technology.

Nanoparticles (NPs) and biomolecules (e.g. DNA, proteins) have nanosized comparable dimensions and there is increasing research interest towards their integration into hybrid nanoarchitectures to synergistically exploit the optical and electronic properties of the first ones with the molecular recognitions capability of the second ones.[1]Among biomolecules, DNA is the most employed biomaterial in the engineering of molecular architectures, for its specificity in molecular recognition, structural versatility and reversibility of interaction.[2]

In 1996 Mirkin[3] reported one of the first pioneering and seminal approaches in the building of molecular nanoarchitectures by coupling nanostructures to DNA. Gold nanoparticles (AuNPs) (13 nm in diameter) were assembled through DNA double strands in macroscopic aggregates, and optical, electronic, and structural properties were finely tuned by varying the number of complementary bases. This research emphasized the potentials of nanostructures as biodetection agents and it represents the starting point for the nanomaterials applications to biodiagnostic and nanomedicine both in homogeneous and heterogeneous detection systems conducted in the following two decades.[4]

Recently much consideration was devoted also to the investigation and tuning of optical properties for plasmonic biosensing and biodiagnostics both in homogenous (LSPR-assay[5]) and in heterogonous detection through the building of nanoarchitectures (and/or nanostructuring) on metallic surface of optical devices (e.g. SERS, Surface Enhanced Raman Spectroscopy[5a,6]and SPR, Surface Plasmon Resonance technology[7]).

Inspiring reviews have been recently published on Surface Plasmon Resonance (SPR) and Surface Plasmon Resonance imaging (SPRi) applied to DNA sensing mediated by metal nanoparticles to improve biosensing performances[8]in molecular diagnostics field.[9] Gold nanoparticles (AuNPs),[10] 10-15 nm in diameter, result the first and the most commonly employed NPs in signal enhancement strategies for ultrasensitive detection thanks to their physico-chemical properties: i.e., higher refractive index variation than the commonly used dielectric materials, size variation and the electromagnetic coupling between Surface Plasmon (SPs) of gold chip surface and electric field of Localized Surface Plasmons (LSPs).[8]Two approaches are generally proposed to improve the performances (i.e. sensitivity) in SPR and SPRi biosensing by using NPs: the secondary enhancement of the signal through the formation of hybrid NPs/DNA nanoarchitectures(e.g. in sandwich-like assays) and the biochip surface nanostructuring.[11]

In literature, one of the first examples of the first strategy is reported by He et al. in 2000 for the detection of complementary DNA sequences (24-mer target) by a home-built SPRi transducer.[12] Afterwards, Corn and coworkers tested sandwich-like assays involving enzymes (i.e. ligase, DNA and RNA polymerase) coupled to DNA/AuNPs sequences hybrids exploited to enhance the analytical signal.[13]More recently, Spoto and coworkers aimed at detecting fully complementary or mismatching sequences in unamplified DNA by coupling the AuNPs-enhanced detection to PNA (i.e. peptide nucleic acids PNA) probes and lowering at the most the detection limits in unamplified plant (zM) and human (aM) genomic sample. [14]

In agreement with our previous research on SPRi biochip surface nanostructuring, where we tested that varying the NPs chemico-physical properties the SPRi biosensing performances changed,[15] we intend here to rationalize, for the first time, how the embedding of different synthesized NPs in hybrid DNA/NPs plasmonic nanoarchitectures (on SPRi chip) influenced the Reflectivity Variation % (%RV), using SPRi technology as test bench and providing a first guideline for the design of amplification assay based on nanoparticles, increasingly used in bioanalytical field. To this aim, three different NPs (silica nanospheres, gold nanospheres, and silver nanoplates) have been rationally chosen to obtain the splitting of some key contributions to the enhancement of the %RV, i.e., refractive index, size and plasmonic profile. The properties are reported in Tab. 1 while details on the NPs synthesis are given in the Electronic Supplementary Information (ESI).

Refractive indexes are computationally evaluated at 635 nm (instrumental source wavelength) with the free online resource http://refractiveindex.info.All the NPs have been characterized by SEM (ESI).

Tab. 1 Properties of the synthesized NPs

NPs	Materials	Shape	Dimension ± SD (nm)	Volume (nm^3)	Refractive index (n)	λmax	Synthesis
Gold nanosphere	Au	Sphere	24 ± 3 (diameter)	7.2 ± 2.7 x 10^3	0.19	528 nm	10a
Silver nanoprism	Ag	Triangular plates	37 ± 4 (side)	3.0 ± 1.0 x 10^3	0.13	633 nm	16
Silica nanosphere	SiO_2	Sphere	113 ± 12 (diameter)	7.6 ± 2.4 x 10^5	1.56	No plasmon	17

Signal enhancement caused by metal NPs can be ascribed to three main contributions: the local change of the refractive index, the influence of NPs size and the plasmonic coupling between SPs and electric field of LSPs of NPs. Gold nanospheres and silver nanoprisms have been selected since they display plasmonic absorbance peaks at 528 nm and 633 nm, far and close, respectively, to the wavelength of the light source (635 nm).Thus the effect of matching peaks between light source and NPs plasmonic excitation on the %RV can be analyzed. On the other hand, silica nanospheres were selected for the absence of any absorption in the visible range, so that any enhancement of the %RV can be ascribed to the sole local refractive index.. While Au nanospheres have been frequently reported coupled to DNA-based measurements by SPRi technology,[11b] to our knowledge this is the second application with silica nanospheres[18] and the first one with silver nanoplates. The modification of pristine metallic NPs is achieved by the well-established functionalization widely reported in literature with a thiolated DNA probes (i.e. 22 mer, namely Probe2).[19] Silica NPs were instead first chemically modified with 1,4-Bismaleimidobutane (1-4 BMB), which is then used to anchor the same thiolated probe. The functionalization of silica nanospheres has been monitored by the change of the surface charge: the Zeta potential before functionalization (-46.52 mV) significantly changed after the functionalization with Probe2 (- 22.88 mV). The NPs/probe incubation conditions were optimized to obtain a DNA probe surface density of 1 Probe/nm^2 for all the NPs types to equalize contingent differences in steric hindrance effects and to prevent unspecific interactions between uncovered gold of NPs and gold biochip surface during the formation of the nanoarchitecture. Experimental conditions and scheme about Probe2@NPslabeling are given in ESI.

After NPs DNA-labeling, a plasmonic nanoarchitecture anchored to the SPRi gold biochip (Fig. 1) and based on a three steps sandwich-like assay is built as it follows: the SPRi bare gold chip is modified by immobilizing the DNA probe (Probe1, black) by exploiting the thiol modification at its 5' end; the hybridization between Probe1 and the Target (84 mer, blue) is performed leading to the complementary DNA duplex; the injection of a NPs type functionalized with Probe2 (red) to hybridize the Target in a different and free region respect to Probe1. The Target sequence belongs to the MDR1 gene, strategic in pharmacogenomics, and here taken as model to highlight possible biodiagnostic applications.[20] Probe1 and Probe2 sequences have been previously selected by OligoWiz 2.0[21]among the most performing probes selectable in term of selectivity[22]. In addition the selectivity of Probe1 was confirmed in a work previously published by our group working with whole unamplified genomic DNA extracted from human blood, but without the use of nanoparticles[22].

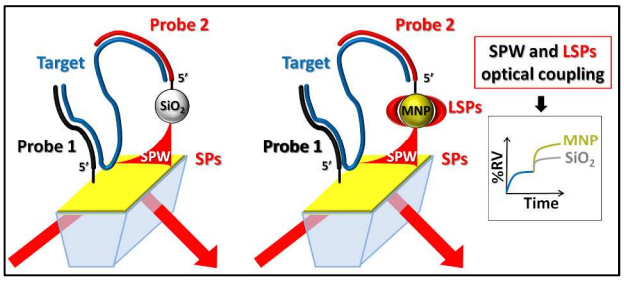

Fig.1 Sketch of the molecular architecture for the evaluation of %RV with different NPs. Thiolated Probe 1 is immobilized on the gold sensing surface. The Target (complementary to Probe 1) is subsequently hybridized to Probe1 and finally the different Probe2@NPs are added to the pre-formed hybrid in separate experiments. The effect of NPs size and material on Reflectivity Variation % is evaluated, splitting the refractive index (n) contribution from the electromagnetic coupling (i.e., LSPs and Surface Plasmon Wave, SPW) one. In particular silica (SiO_2) nanospheres without absorption in the visible range, Au nanospheres with a plasmon absorbance profile not matching that of the gold chip, and Ag nanoprisms with a plasmon absorbance profile matching that of the gold chip were synthesized and tested.

Results obtained, expressed as %RVs and visualized by digital images of Probe2@NPs binding, are reported Fig. 2 for each examined case (a, b, and c columns). %RV signals reported in bars (a, b and c columns) are relative only to the secondary hybridization of Probe2@NPs on the Target sequence, since we focus on the effect of the different NPs properties within the evanescent wave and how this influences the resonance state and then the %RV recorded. A control probe (CProbe), sequenced from EGFP1 gene (not human origin) is separately immobilized as spot on the same biochip to check that any molecular recognition recorded on the Probe1 was only due to the complementary base pairings and not to other unspecific interactions such as electrostatic interactions and/or NPs collapsing on the gold surface. All the DNA sequences are reported in Tab. 1 of ESI. %RVs are recorded by SPRi-Lab$^+$ from Horiba Scientific (Orsay, France) at a fixed angle of incident light (635 nm). Instrumental details and experimental conditions are reported in ESI.

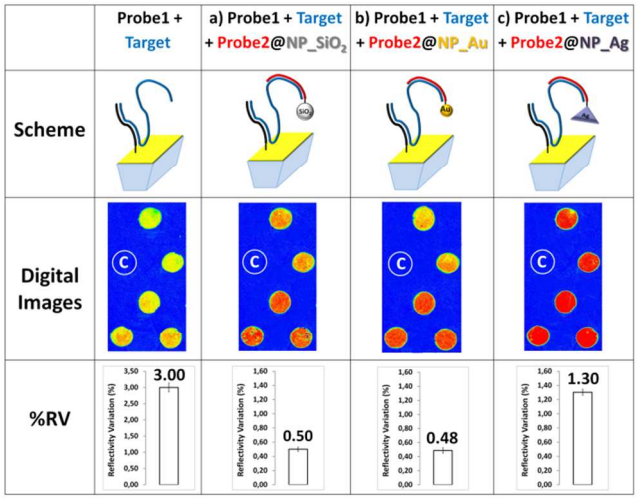

Fig. 2 Scheme, digital images and reflectivity variation % (%RV) of the target hybridization and a) Probe2-functiolized gold nanospheres, b) Probe2-functionalized silver nanoplates, and c) Probe2-functionalized silica nanospheres hybridizations (Zoomed Fig.2 is reported in Fig.4A in ESI).

As result the %RV recorded from the hybridization of 250 nM Target (3.00 ± 0.14 %RV) emphasize a good repeatability (%CV = 4.7%). In ESI (Fig. 3A) a calibration curve has been also reported at decreasing Target concentrations for the evaluation of the DL. Digital images and %RV signals of the Probe2@NPs highlight that the highest %RVs is recorded when Probe2 labelled to silver nanoplates (1.30 ± 0.04 %RV, %CV=3.1%) hybridize to the Target, obtaining a signal increment of ~ 2.7-fold compared to silica (0.50 ± 0.04 %RV, %CV = 8.0%) and gold (0.48 ± 0.06 %RV, %CV = 12.5%) nanospheres. However with all three NPs a good repeatability was recorded (%CV < 13%).

Thanks to the rational choice of shape and material of NPs it is then possible to evaluate the main contributions of refractive index, size and plasmons couplings.

In 2003 Homola[23] reported that, according to the perturbation theory, if the binding occurs within the depth of the Surface Plasmon Wave (SPW) field, it would induce a refractive index change Δn (between bulk media and binding species) proportional to the change of the real part of the propagation constant, Δβ, (Re{Δβ} □kΔn), causing the %RV.

As reported by Yunuset al.[24] the refractive index of sodium chloride (main salt in the PBS solution) at 300 mM concentration, ~ 1.8 % (%w/w), our salt concentration, (see Experimental Supporting Information) in water solution and measured at 633 nm (really close to our source wavelength, 635 nm) is approximately 1.33 (nPBS). Since Probe2 is immobilized on the NPs with the same maximum achievable surface density (1 probe/nm^2) for each NPs type its contribution to the refractive index can be overlooked. Thus the contribution to changes of the real part of the propagation constant (Δβ) can be directly estimated from the difference between the refractive index of the PBS solution (nPBS) and that relative to the contribution due to the NPs in solution. Since the refractive indexes of gold and silver NPs, computationally evaluated by http://refractiveindex.info.com[25](at 635 nm, source wavelength) result respectively nAu = 0.19 and nAg = 0.13 (Tab. 1), we can infer that in these conditions we have: ΔnPBS-Ag |1.33-0.13|= 1.20 for AgNPs, and ΔnPBS-Au |1.33-0.19|=1.14 for AuNPs. Therefore, the ratio between the two differences brings to an increase of 5.3%, not sufficient to explain a %RV enhancement of ~ 2.7-fold, as reported by the signals in the Fig. 2.

Spoto and Minunni[8c] report that signal increases can be also explainable by the size enhancement of the NPs and Springer et al.[26] recently found, in good agreement to theoretical models, that the sensitivity to surface density (nm/μm^2) of spherical gold NPs increases with the diameter.

Since the volume (Tab. 1) of Au nanospheres (7.2 ± 2.7 x 10^3 nm3) is ~ 2.4-fold greater than the Ag triangular equilateral nanoplates (3.0 ± 1.0 x 10^2 nm^3) one, we can infer that the signal enhancement obtained with AgNPs does not derive from their size, supporting the hypothesis that the key parameter is the plasmons coupling between SPs and electric field of LSPs occurring from the matching of source wavelength (635 nm) and the maximum plasmonic excitation of the silver nanoplates one (633 nm).

A similar discussion can be undertaken for silica nanospheres, having a refractive index (nSiO_2 = 1.56) closer to the PBS solution (nPBS = 1.33) than Ag nanoprisms (nAg = 0.13), but with much larger dimensions (5.24 x 10^5 nm3, ~ 600-fold the mass of Ag nanoprisms). The corresponding %RV recorded with silica NPs (0.50%, Fig. 2) emphasizes therefore that the effect of their dimensions on signal enhancement is, in our conditions, by far less crucial than the existence of an effective plasmonic electromagnetic coupling between LSPs and SPs. To confirm this hypothesis we have normalized the %RVs recorded for each NPs type compare to the corresponding volume (nm^3). In this way we find that SiO_2nanospheres can elicit 6.58 x 10^{-7} %RV/nm^3, Au nanosphers 6.67 x 10^{-5} %RV/nm^3, and Ag nanoplates 4.66 x 10^{-4} %RV/nm^3 respectively. This can be transduced in a ~7-fold normalized signal gain (%RV per nm^3) with Ag nanoplates compared to Au nanospheres and ~ 700-fold to SiO_2nanospheres. All these findings clearly point the importance of matching the source wavelength (635 nm) to the NPs plasmon absorption wavelength peak. Indeed, only thanks to the peculiar optical properties of silver nanoprisms (plasmon absorption peak = 633 nm) it is possible to invoke a resonance of gold chip SPs with LSPs of Ag NPs, generating a higher %RV than the other NPs ones. In the case of gold nanospheres, the distance between the wavelengths for Au peak of absorption (528 nm) and the source light emission (635 nm) can explain the lower effect (or absence) of plasmon coupling leading to a lower %RV variation. Similarly, for silica nanospheres (where no plasmon resonance could be excited) the sole effect resulting from their dimensions is not sufficient for a comparable %RV enhancement.

In addition, each digital image recorded in Fig. 2 clearly shows the specificity of the biomolecular recognition: in fact, no unspecific interaction is detected on the gold surface and control (C). In Fig. 3 the sensorgram (%RV vs Time) of the two steps in nanoarchitecture formation with DNA-labeled Ag nanoprisms is reported. The nanoarchitectureis reversible by the simple injection of a chaotropic agent(e.g. 10mMNaOH solutions) for 30 seconds, highlighting once again the absence of unspecific interactions on the gold surface and opening new horizons for possible biosensing applications where chip regeneration is mandatory for daily routine and cheap applications.

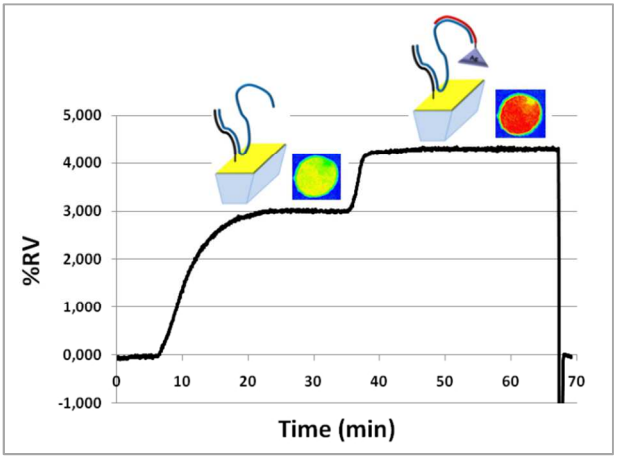

Fig.3 Sensorgram of the hybridization of Target to Probe1 (first %RV variation) and Probe2 labeled with silver nanoprisms in the sandwich-like assay, together with relative digital images of one spot. Regeneration was performed with 10mMNaOH at 300 μl/min flow rate for 30 s.

The study presented here is one the first attempts in the rational investigation of the single contribution of refractive

index, size, and plasmonic profiles of NPs applied to SPRi technology with suitable biosensing applications. We here demonstrate that the optimal resonance condition achievable by the coupling of SPs and LSPs of NPs occurs in presence of overlapping between source wavelength and LSPs wavelength of maximum excitation, and that the contribution of this to %RV is more crucial than refractive index and size ones. These findings results really helpful to design a signal amplification assay based on nanoparticles since it provides a guideline to reach a more efficient plasmon coupling with a resulting improvement in %RV signals. We have performed the study on a plasmonic nanoarchitecture based on a DNA/DNA sandwich assay whose selectivity and reliability for clinical and diagnostic applications has already been tested (without nanoparticles) [22, 27].In perspective, we are confident that further progress can result from the exploration of other shapes, sizes, dimensions and materials,[2a] studying and tuning optical properties to maximize the phenomenon of plasmon couplings, with resulting sensitivity improvements for DNA biosensing applications in the field of biodiagnostics and nanomedicine.

Notes and references

[a]*Dipartimento di Chimica "Ugo Schiff", Università di Firenze, Via della Lastruccia 3-13, 50019 Sesto Fiorentino (FI), Italy;Tel: 0554573314;*
[b]*Consorzio dei Sistemi a Grande Interfase (CSGI), Università di Firenze, Via della Lastruccia 3-13, 50019 Sesto Fiorentino (FI), Italy;Tel: 0554573014;*
*massimo.bonini@unifi.it; bonini@csgi.it; maria.minunni@unifi.it

† Electronic Supplementary Information (ESI) available: [details of any supplementary information available should be included here]. See DOI: 10.1039/b000000x/

1 a) E. Katz and I. Willner, *Angew. Chem. Int. Ed. Engl.*, 2004, **43**, 6042. b) X. Lan and Q. Wang, NPG Asia Mater, 2014, 6, e97. c) X. Lan, Z. Chen, G. Dai, X. Lu, W. Ni, and Q. Wang, J. Am. Chem. Soc., 2013, 135, 11441–11444.

2 a) S. J. Tan, M. J. Campolongo, D. Luo, and W. Cheng, *Nat Nano*, 2011, **6**, 268–276; b) X. Lan, X. Lu, C. Shen, Y. Ke, W. Ni, and Q. Wang, J. Am. Chem. Soc., 2015, **137**, 457–462.

3 C. A. Mirkin, R. L. Letsinger, R. C. Mucic, and J. J. Storhoff, *Nature*, 1996, **382**, 607–609.

4 (a) C. S. Thaxton, D. G. Georganopoulou, and C. a Mirkin, *Clin. Chim. Acta.*, 2006, **363**, 120. (b) H. Jans and Q. Huo, *Chem. Soc. Rev.*, 2012, **41**, 2849. (c) E. Boisselier and D. Astruc, *Chem. Soc. Rev.*, 2009, 38, 1759–1782. (d) L. Dykman and N. Khlebtsov, *Chem. Soc. Rev*., 2012, 41, 2256.

5 (a) P. D. Howes, S. Rana, and M. M. Stevens, *Chem. Soc. Rev.*, 2014, **43**, 3835. (b) S. Szunerits and R. Boukherroub, *Chem. Commun. (Camb).*, 2012, **48**, 8999. (b) K. E. Fong and L.-Y. L. Yung, *Nanoscale*, 2013, **5**, 12043. (c) G. K. Joshi, P. J. McClory, S. Dolai, and R. Sardar, *J. Mater. Chem.*, 2012, **22**, 923–931.

6 (a) J. N. Anker, W. P. Hall, O. Lyandres, N. C. Shah, J. Zhao, and R. P. Van Duyne, *Nat. Mater.*, 2008, **7**, 442. (b) H.-I. Peng and B. L. Miller, *Analyst*, 2011, **136**, 436; c) X. Lan, Z. Chen, X. Lu, G. Dai, W. Ni, and Q. Wang, ACS Appl. Mater. Interfaces, 2013, 5, 10423–10427.

7 J. Homola, *Chem. Rev.*, 2008, **108**, 462; X. Lan, Z. Chen, B.-J. Liu, B. Ren, J. Henzie, and Q. Wang, Small, 2013, 9, 2308–2315.

8 (a) R. D'Agata and G. Spoto, *Anal. Bioanal. Chem.*, 2013, **405**, 573. (b) H. Šípová and J. Homola, *Anal. Chim. Acta*, 2013, **773**, 9. (c) G. Spoto, M. Minunni, *J. Phys. Chem. Lett.*, 2012, **3(18)**, 2682.

9 (a) S. Mariani and M. Minunni, *Anal. Bioanal. Chem.*, 2014, **406**, 2303. (b) M. L. Ermini, S. Mariani, S. Scarano, and M. Minunni, *Biosens. Bioelectron.*, 2014, **61C**, 28.

10 (a) J. Turkevich, P. C. Stevenson, and J. Hillier, *Discuss. Faraday Soc.*, 1951, **11**, 55–75. (b) K. Saha, S. S. Agasti, C. Kim, X. Li, and V. M. Rotello, *Chem. Rev.*, 2012, **112**, 2739.

11 (a) M. E. Stewart, C. R. Anderton, L. B. Thompson, J. Maria, S. K. Gray, J. A. Rogers, R. G. Nuzzo, *Chem. Rev*.2008, **108**, 494. (b) E. E. Bedford, J. Spadavecchia, C. Pradier, and F. X. Gu, *Macromol. Bio*.,2012, **12**, 724.

12 L. He, M. D. Musick, S. R. Nicewarner, F. G. Salinas, S. J. Benkovic, M. J. Natan, C. D. Keating, R. April, *J. Am. Chem. Soc.*, 2000, **122**, 9071.

13 (a) Y. Li, A. W. Wark, H. J. Lee, R. M. Corn, *Anal. Chem*., 2006, **78**, 3158. (b) S. Fang, H. J. Lee, A. W. Wark, R. M. Corn, *J. Am. Chem. Soc.* 2006, **128(43)**, 14044. (c) I. E. Sendroiu, L. K.Gifford, A. Lupták, R. M. Corn, *J. Am. Chem. Soc.* 2011, **133(12)**, 4271.

14 (a) R. D'Agata, R. Corradini, C. Ferretti, L. Zanoli, M. Gatti, R. Marchelli, G. Spoto, *Biosens. Bioelectron.* 2010, **25**, 2095. (b) R. D'Agata, G. Breveglieri, L. M. Zanoli, M. Borgatti, G. Spoto, R. Gambari, *Anal. Chem.*, 2011, **83**, 8711.

15 S. Mariani, M. L. Ermini, S. Scarano, F. Bellissima, M. Bonini, D. Berti, and M. Minunni, Microchim. Acta, 2013, **180(11-12)**, 1093.

16 Aherne, D., Ledwith, D.M., Gara, M., and Kelly, J.M., 2008. *Adv. Funct. Mater.***18**, 2005.

17 M. Nakamura and K. Ishimura, *Langmuir*, 2008, **24**, 5099.

18 W.-J. Zhou, A. R. Halpern, T. H. Seefeld, and R. M. Corn, *Anal. Chem.*, 2011, **84**, 440.

19 (a) A. Steinbrück, Csaki, K. Ritter, M. Leich, J.M. Köhler, W. Fritzsche, *J. Biophotonics,* 2008, **1**, 104.(b) L.M. Zanoli, R. D'Agata, and G. Spoto, *Anal. Bioanal. Chem*. 2012, **402**, 1759.

20 C. Marzolini, E. Paus, T. Buclin, and R. B. Kim., *Clin. Pharmacol. Ther.,* 2004,**1**, 13.

21 R. Wernersson, A. S. Juncker, and H. B. Nielsen, *Nat. Protoc*., 2007, **2**, 2677.

22 M. L. Ermini, S. Mariani, S. Scarano, and M. Minunni, Biosens. Bioelectron., 2013, 40, 193.

23 J. Homola,. *Anal. Bioanal. Chem.,* 2003, **377**, 528.

24 W.M. Yunus and A.B. Rahman, *Appl Opt.*, 1988 15;27(16):3341.

25 M. N. Polyanskiy. Refractive index database, http://refractiveindex.info. Accessed Ott. 28, 2014.

26 T. Špringer, M. L. Ermini, B. Špačková, J. Jabloňků, and J. Homola, *Anal. Chem*., 2014, **86**, 10350.

27 (a) M. L. Ermini, S. Mariani, S. Scarano, D. Campa, R. Barale, and M. Minunni, Anal. Bioanal. Chem., 2013, **405**, 985. (b) S. Mariani, S. Scarano, M. Carrai, R. Barale, M. Minunni, *Anal. Bioanal. Chem.*, 2015,. DOI: 10.1007/s00216-014-8424-1.